

A Supervisory Volt/VAR Control Scheme for Coordinating Voltage Regulators with Smart Inverters on a Distribution System

Valliappan Muthukaruppan, *Student Member, IEEE*, Yue Shi, *Member, IEEE*,
and Mesut E. Baran, *Fellow, IEEE*

Abstract—This paper focuses on the effective use of smart inverters for Volt/Var control (VVC) on a distribution system. New smart inverters offer Var support capability but for their effective use they need to be coordinated with existing Volt/Var schemes. A new VVC scheme is proposed to facilitate such coordination. The proposed scheme decomposes the problem into two levels. The first level uses Load Tap Changer (LTC) and Voltage Regulators (VRs) and coordinates their control with smart inverters to adjust the voltage level on the circuit to keep the voltages along the circuit within the desired range. The second level determines Var support needed from smart inverters to minimize the overall power loss in the circuit. The results of the supervisory control are sent to the devices which have their local controllers. To avoid frequent dispatch, smart inverters are supervised by shifting their Volt/Var characteristics as needed. This allows for the smart inverters to operate close to their optimal control while meeting the limited communication requirements on a distribution system. A case study using the IEEE 34 bus system shows the effectiveness of this supervisory control scheme compared to traditional volt/var schemes.

Index Terms—Volt/Var Optimization, Coordinated Control, Smart Inverters, Volt/Var Curve

I. INTRODUCTION

Current Volt/VAR Control (VVC) schemes implemented by many utilities use legacy control devices such as capacitor banks, load tap changers and voltage regulators. The primary goal is to keep the voltage across the feeder within the ANSI limit [1]. Recent increase in deployment of distributed energy resources (DERs) on distribution system challenges effectiveness of the conventional VVC schemes [2]. On the other hand, it was recognized that the inverters used in most DERs can provide Var support. To encourage the use of this new capability, IEEE Std. 1547 has been revised and new operating modes with varying Volt-Var characteristics (VVar-C) have been developed for these new smart inverters (SI) [3]. However, for the SIs to be effective in supporting VVC, their VVar-Cs need to be chosen very carefully and need to be updated as system conditions change [4].

VVar-C based control for SIs is a popular local control framework which has been adopted by IEEE 1547 standard [3] and adopted by Rule-21 in California [5]. In [6], the author points out that the local control is effective in mitigating the

voltage rise issue due to high PV penetration, but also points out the oscillatory problem even for single SI with droop control scheme. In [4], the author addresses the low steady state error (SSE) and stability/convergence issues associated with droop control by dynamically adapting the droop parameters. In [7] a VVC scheme using legacy devices is proposed, and it incorporates SIs with fixed VVar-C.

An alternative approach is to treat SIs as Var dispatchable sources and formulate the problem as Optimal Power Flow (OPF) problem [8], [9], [10]. To address the computational challenges, two control loops with different timescales are proposed in [11], [12]. In the slow update loop, the legacy devices are dispatched, and in the fast update loop, SIs are dispatched by solving a separate Var optimization problem. In this approach, the large number of discrete variables needed to represent VR operation increases the computational burden significantly. To address this issue, we propose an efficient search algorithm for finding optimal tap positions of VRs.

Another challenge in implementing an OPF based scheme is that sending the dispatching signals frequently which may not be feasible with the limited communication infrastructure at distribution level [13], [14], [15].

This paper addresses these issues by introducing a new coordinated VVC scheme which adjusts the Volt-Var settings of SIs periodically rather than sending Var commands directly. Also, a computationally efficient method for the VVC method is proposed to facilitate its implementation in the field. This method also keeps legacy device operations low by making use of the fast-acting capability of smart inverters. The main contribution of this paper are as follows:

- VVC problem as a version of optimal power flow problem is NP-hard. There have been methods proposed based on convex relaxation of the original non-convex problem [16], [17] that can find global optimal solution under certain system conditions but they cannot handle discrete or integer variables associated with LTC and VR control [18]. On the other hand, linearizing the original power flow problem allows incorporation of LTC/VR control thereby allowing full coordination between the devices but the number of discrete variables introduced by LTC/VR control increases exponentially and may not be feasible for large systems [12]. To address these issues we propose a two-stage scheme. The first stage determines the set points for LTC, VR devices, and smart inverters by using an efficient search algorithm for VR/LTC tap

Corresponding Author: Mesut Baran (baran@ncsu.edu)

The authors are with Department of Electrical and Computer Engineering, North Carolina State University, Raleigh, NC 27695 USA (email: vmthuk2@ncsu.edu, yueshi0430@gmail.com, and baran@ncsu.edu)

settings. This provides a proper coordination between these devices and assures that voltages in the system will be within desired limits while keeping the number of tap changes low compared to conventional VVO schemes. The second stage checks if the Var dispatch for SIs can be further adjusted to decrease the power loss.

- To address the limited communication infrastructure available in field, we propose a new dispatching scheme for sending optimal Var commands to SIs through shifting of their volt/var curves. This scheme ensures that the smart inverters will continue to inject reactive power close to optimal value in between the dispatch intervals and provide additional fast response when there is intermittency from DERs.

The rest of the paper is organized as follows. In section II, we propose the coordination strategy for dispatching LTC/VR and smart inverters simultaneously and in section II-B we propose the shifting curve strategy for smart inverter dispatch to avoid the frequent dispatch problem. The performance of proposed control is then evaluated using a test system in section III.

II. SUPERVISORY VVO

The application considered here is the VVC scheme to be implemented by a utility on a distribution system with SIs. The proposed VVC scheme (i) coordinates the operation of SIs with the utility Volt-Var devices, and (ii) is computationally efficient for easy adoption in practice.

A central VVC scheme will be most effective in this case to assure proper coordination between the utility VVC and SIs. The dispatch speed for the controller is a critical issue at distribution level, as utilities generally utilize a radio-mesh/cellular based communication infrastructure in distribution system. On the other hand, high intermittency DERs necessitates that the dispatch needs to be as fast as possible. In this work, it is assumed that utility has a good distribution SCADA which can collect data from the field for the control cycle.

The proposed scheme which is central will supervise both the conventional VVC devices and the SIs which can be controlled by the utility for additional Var support. To reduce the computational burden, we adopt a two-stage optimization scheme shown in fig. 1. As the figure indicates, stage-1 utilizes smart inverters and LTC/VRs to find a feasible operating point preparing for stage-2 which utilizes smart inverters to minimize the total power loss in the circuit. This approach allows SIs to respond to voltage violations first, thus avoiding unnecessary adjustments of VRs. These two stages are elaborated below.

A. Stage-1: Feasible Operating Point

The goal of stage-1 is to bring the voltages well within the desired limits. To minimize the use of legacy devices which can be subject to mechanical wear and tear with frequent operation, we utilize SIs first to bring the voltage within ANSI limits ($v \in [0.95, 1.05]$ p.u.) and only if the inverters hit their power limits or voltage violations still exist after using inverters we use LTC/VR to regulate the voltage.

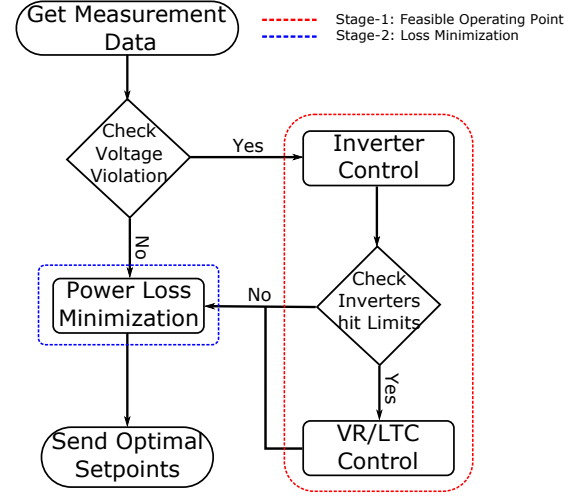


Fig. 1. Flowchart of proposed algorithm

1) *Inverter Control*: The objective of inverter control in stage-1 is to flatten the voltage across the system. Let $g(v, q)$ denote the power flow constraints which is a set of equations $\forall i \in \mathcal{N}$ given by (1) and (2) where \mathcal{N} is the set of system nodes.

$$p_i^g - p_i^l = v_i \sum_{j \in \mathcal{N}} v_j (G_{ij} \cos \theta_{ij} + B_{ij} \sin \theta_{ij}) \quad (1)$$

$$q_i^g - q_i^l = v_i \sum_{j \in \mathcal{N}} v_j (G_{ij} \sin \theta_{ij} - B_{ij} \cos \theta_{ij}) \quad (2)$$

Here, p_i^g is the real power generation from PV at node i , p_i^l is the real power consumption at node i , q_i^g is the reactive power injection from smart inverters, and q_i^l is the reactive power consumption. $\theta_{ij} = \theta_i - \theta_j$ is the voltage difference between node i and j , $G_{ij} + jB_{ij} = Y_{ij}$ is the element of Y-bus matrix. The mathematical formulation of this problem is given in (3) which is solved using a gradient-descent approach.

$$\begin{aligned} \min_{q^g} \quad & \sum_{i \in \mathcal{N}} \omega_i (v_i - v_{ref})^2 \\ \text{s.t.} \quad & g(\mathbf{v}, \mathbf{q}) = 0, \\ & v_{min} \leq v_i \leq v_{max} \quad \forall i \in \mathcal{N}, \\ & q_{min}^g \leq q_i^g \leq q_{max}^g \quad \forall i \in \mathcal{N}, \\ \text{where,} \quad & \begin{cases} \omega_i = 0 & \text{if } v_i \in [0.95, 1.05] \\ \omega_i = 1 & \text{otherwise} \end{cases} \end{aligned} \quad (3)$$

Here, v_{ref} is the desired voltage profile through out the system, generally fixed at 1.0 p.u. \mathbf{v} is the vector of voltage magnitudes and \mathbf{q} is the vector of reactive power injections.

2) *VR/LTC Control*: As indicated earlier LTC/VR control is only utilized when the inverters are unable to regulate the voltage. The LTC and VR tap positions are discrete; these devices usually have 33 taps (including the zero-tap position) and each tap corresponds to a 0.00625 p.u. voltage change. The LTC at substation is typically three-phase gang-operated, while the VRs are usually controlled on a phase basis to be able to adjust voltage on each phase independently.

Due to discrete tap control, an exhaustive search for feasible tap settings can be computationally challenging. With R single

phase controlled regulators and K three phase controlled regulators, the total search space will be 33^{3R+K} . For example, a system with one LTC and one VR, total possible tap combinations will be $33 \times 33 \times 33 \times 33 = 1,185,921$. To reduce the search, a search method based on [19] has been developed. The method is based on the observation that most of the time tap adjustments needed are small. Hence, instead of searching all possible 33 taps, the method reduces the feasible search space to at most 2 to 3 taps up or down, $\Delta Tap = \{0, \pm 1, \pm 2, \pm 3\}$.

In this work we further reduce this search space by applying additional rules as given in fig. 2. As the figure shows, voltages are calculated by varying the voltage control device closest to the substation (e.g. LTC) with tap adjustment $Tap_{LTC}(k) \in \Delta Tap$, while keeping tap position constant for downstream voltage control devices. If over-voltage violations occur, only down taps of downstream devices are searched. If under-voltage violations occur, only up taps of downstream devices are searched. In fig. 2, p represents the corresponding phase of voltage regulator. We use a backward-forward three-phase distribution power flow solver to determine the voltages for different tap combinations during the search. This approach reduces the overall search space to $3^{3R} + K$ on average and $7^{3R} + 3^K$ on worst case.

Since there will be many tap settings that will bring the voltages within the limits, a criterion is needed to determine the preferred settings for the legacy devices. In our scheme, keeping the voltage profile as flat as possible is selected as the criteria, as this is the preferred voltage profile for a feeder. Hence, in the search, the feasible VR settings are ranked using the voltage variance criterion as shown in (4), and after the search the VR tap settings with best voltage profile is selected as the new tap settings for VRs. The V_{ref} is generally chosen as 1.0 p.u. and having a flat voltage profile can lead to lower power loss and power consumption in the circuit through Conservation Voltage Reduction (CVR) [12].

$$V_{var} = \sum_{i \in \mathcal{N}} (V_i - V_{ref})^2 \quad (4)$$

B. Stage-2: Loss Minimization

The objective in this stage is to optimally dispatch the reactive power injections of SIs to minimize the total power loss in the circuit while keeping the voltages within limits. The mathematical formulation of this problem is given in (5) which is also solved using a gradient-descent approach:

$$\begin{aligned} \min_{q^g} \quad & \sum_{i \neq j} G_{ij} [v_i^2 + v_j^2 - 2v_i v_j \cos \theta_{ij}] \\ \text{s.t.} \quad & g(\mathbf{v}, \mathbf{q}) = 0, \\ & v_{min} \leq v_i \leq v_{max} \quad \forall i \in \mathcal{N}, \\ & q_{min}^g \leq q_i^g \leq q_{max}^g \quad \forall i \in \mathcal{N}, \\ \text{where,} \quad & \begin{cases} \omega_i = 0 & \text{if } v_i \in [0.95, 1.05] \\ \omega_i = 1 & \text{otherwise} \end{cases} \end{aligned} \quad (5)$$

C. Dispatching of Smart Inverter

The set points obtained by VVO need to be dispatched to the SIs on the system. Due to limited communication

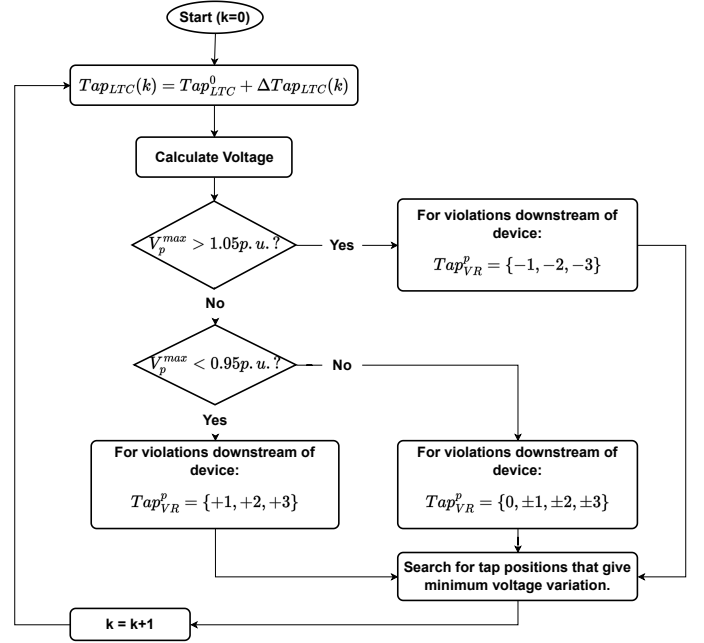


Fig. 2. Flowchart of VR/LTC Module

infrastructure and bandwidth utilities are unable to dispatch optimal var commands to inverters frequently. On the other hand, relying completely on local control approach using VVar-C can impact the overall VVO since they follow a fixed VVar-C. The new dispatch strategy we propose for SIs uses the Var settings from VVO and determines how to adjust VVar-C of SIs so that they will provide Var support indicated by VVO during the dispatch period.

The VVar-C is generally characterized by a slope ΔQ and a reference point V_{ref} which is realized using four points $(V_1, Q_1), (V_2, Q_2), (V_3, Q_3)$ and (V_4, Q_4) as shown in fig-3. Where Q_1, Q_4 correspond to Q_{lim} of the inverter and Q_2, Q_3 are generally 0.

In [20], the author disseminates the engineering of local control and provides a framework for perceiving the dynamical nature of VVar-C as a distributed optimization problem that strives to minimize the deviation of system voltage from nominal value (v_{ref}) while simultaneously minimizing the reactive power provisioning required at each inverter.

In [20] the author proves that the equilibrium point of this curve is a unique point (v^*, q^*) which satisfies the power flow equations $g(v^*, q^*)$ and the VVar-C curve $q^* = f(v^*)$. We use this theorem to shift the VVar-C from current curve to new curve based on the optimal solution (v^*, q^*) obtained from the centralized optimization problem. We prove in theorem-II.1 that by shifting the curve, new equilibrium point of the curve after the dynamics will be the optimal set point (v^*, q^*) .

Theorem II.1. Given an optimal power flow solution (v_g, q_g) for any operating point, by shifting the existing volt/var curves $q = f_1(v - v_{ref})$ where $f_1: \mathbf{R}^n \rightarrow \Omega$ is collection of volt/var function of all inverters in the system, along the voltage axis by $v^g - v^l$ where $v^l = f_1^{-1}(q^g)$ is voltage corresponding to q^g on existing volt/var curve f_1 will result in a new set of

volt/var curves f_2 whose equilibrium point will be (v_g, q_g) .

$$q_g = f_2(v_g - v_{ref})$$

where, $f_2(v - v_{ref}) = f_1(v - v_{ref} + v_g - v_l)$ (6)

Proof of theorem-II.1 is provided in Appendix. Suppose say q_g is the optimal solution of a inverter to our centralized problem and v_g be the corresponding voltage at the inverter which implies $g(v_g, q_g) = 0$ since it is also a feasible solution. Now, using the current VVar-C at the inverter we find the voltage v_l that will correspond to the optimal var q_g . Note that (v_l, q_g) is not a equilibrium point of the VVar-C since it does not satisfy the power flow constraints. By shifting the four set points of the curve by $v_g - v_l$, the new equilibrium point will in fact fall at (v_g, q_g) according to theorem-II.1. The direction of shift will be intrinsically handled by the sign of the difference $v_g - v_l$. The dispatching algorithm is explained in algorithm-1 and highlighted in fig. 3.

Algorithm 1 VVar-C Shifting Algorithm

Input: Old VVar-C - $\hat{f}_i(v) \quad \forall i \in \mathcal{N}_{SI}$

Output: New VVar-C - $f_i(v) \quad \forall i \in \mathcal{N}_{SI}$

- 1: Run the centralized optimization problem to obtain the individual var commands q_i^g and the corresponding voltage $v_i^g \quad \forall i \in \mathcal{N}_{SI}$.
 - 2: Obtain the voltage v_i^l corresponding to q_i^g using the old curve $\hat{f}_i(v_i^l)$.
 - 3: Shift the curve by $v_i^g - v_i^l$ which leads to new curve $\hat{f}_i(v_i^l + v_i^g - v_i^l) = f_i(v_i^g)$.
 - 4: With this new curve $f_i(v_i^g)$, the equilibrium point for current operating condition will be (q_i^g, v_i^g) . Dispatch the new curves $f_i(v)$ to the inverters.
-

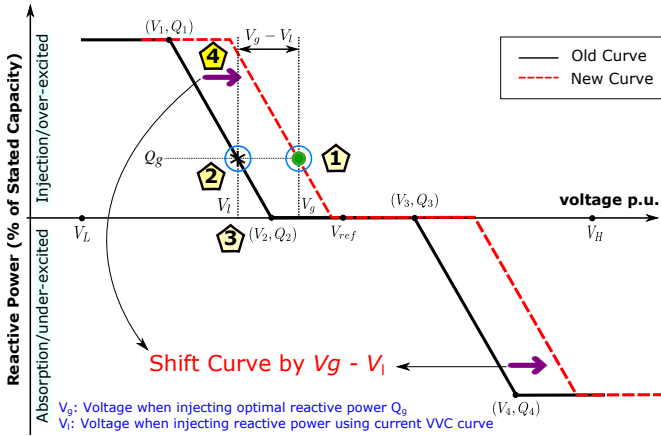


Fig. 3. VVar-C Shifting Strategy

With this framework only the shift in curve $v_g - v_l$ needs to be dispatched to each individual inverter instead of all the four setpoints thereby reducing the communication overhead required. Also, when the q_g is very small (say below 0.1 p.u) then the new curve is not dispatched and that particular inverter is left at old curve to further reduce the communication burden. It is important to note that with this shifting strategy only the

v_{ref} of the inverters are modified but the slope of the VVar-C remains same thereby avoiding any stability issues in the control.

III. CASE STUDY

A modified version of the IEEE 34 node system is utilized for simulating the test cases as shown in fig. 4. This test feeder is based upon an actual feeder in rural Arizona. The transformer between nodes 832 and 888 is removed from the original feeder. A three-phase controlled LTC is installed at the substation and VR_1 is retained at its original location while VR_2 between nodes 852 and 832 is removed. The VR_1 and LTC have ± 16 tap position range with $\pm 10\%$ of maximum voltage change. The three phases of the VRs are controlled separately. All shunt capacitors are removed from the original system. There are 20 nodes with load connected to them in the original 34 node system. We connect 10 nodes with PV system and of these 6 have smart inverter VVar-C capability as highlighted in the figure 4. The 24 hour total load and PV profiles simulated are shown in fig. 5. We evaluate the algorithm against four different operating conditions consisting high load condition in summer, light load condition in winter, cloudy PV day with lot of intermittency in PV output and a clear sunny day with peak PV output.

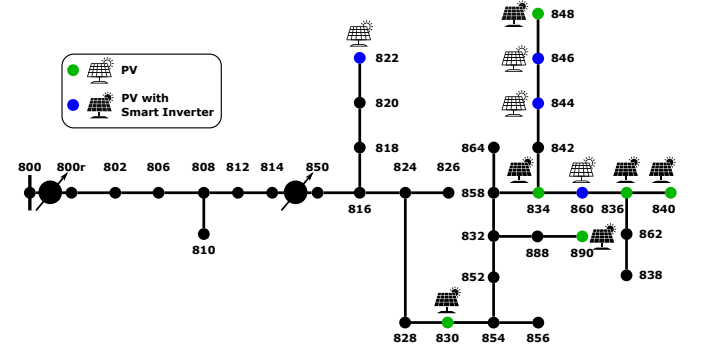


Fig. 4. Test System with Location of PV and Smart Inverters.

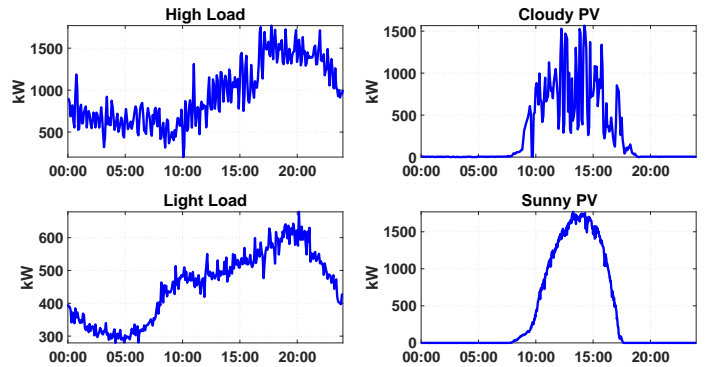


Fig. 5. Load and PV profiles used in the case study.

A. Test Cases

To assess the performance of the proposed scheme three VVC schemes are considered:

- **Case-1:** LTC and VR operate under local control. PV system are present in the circuit but they donot have any smart inverter capability and hence do not provide any VAR support.
- **Case-2:** LTC and VR act under local control. PV system have smart inverter capability and act under local control with a fixed VVar-C curve.
- **Case-3:** Proposed coordinated VVO scheme with coordination between legacy devices and smart inverters. Also the proposed dispatch scheme is used to dispatch VVar-C curves.

1) *Case-1:* In this case, only conventional devices participate in the volt/var control. The control is purely based on local measurements [21]. The LTC and VR control settings are highlighted in table-I.

TABLE I
SET POINTS FOR LEGACY DEVICES

Setting	VR	LTC
V_{set}	120V	122V
Bandwidth	2V	2V
Time Delay	60s	30s
Max tap Change	1	1

Even though PV inverters are shown in fig. 4 they do not participate in the Volt/Var Control. The objective of setting up this case is to show that legacy devices are not capable of restricting voltage violations in presence of high PV.

2) *Case-2:* In this case, apart from the LTC and VR, the smart inverters in the system also participate in the volt/var control. All devices operate based on local measurements and the control strategy of LTC and VR are same as case-1. All the smart inverters here will have a fixed volt/var curve as shown in fig. 6 and operate based on the local voltage measurements at the inverter terminals.

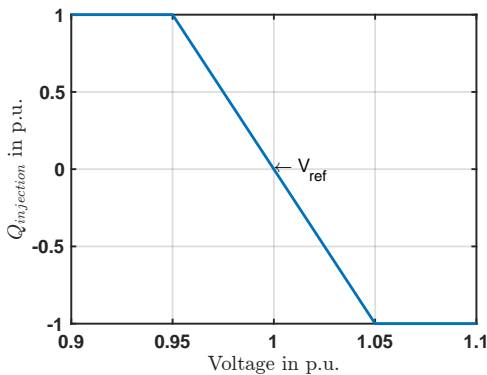


Fig. 6. Default VVar-C for Smart Inverters.

3) *Case-3:* Case-3 is the proposed coordinated VVO with curve shifting dispatch scheme. All inverters are initialized with the fixed curve as shown in fig. 6 but will be shifted based on the optimal var injections obtained from the var optimization module every 5 minutes (assumed dispatch period) and it dispatches tap change commands to legacy devices and the shifted VVar-C to SIs. The smart inverters will use the new VVar-C and the local voltage measurements to inject necessary

reactive power during the sub 5-minute interval. All SIs are initialized with the fixed curve as shown in fig. 6.

As explained in sec-II-B, to avoid frequent shifting of VVar-C a threshold of 10% total var is introduced in the shifting algorithm. Whenever the optimal var injection q_g for an inverter is less than 10% of total var limit of the inverter, the VVar-C is retained at old curve and no shifting is applied to that inverter.

B. Test Results

We use various metrics to evaluate the performance of the proposed VVO scheme. During the 24 hour simulation:

- 1) N_{UV} is the number of under voltage violations.
- 2) N_{OV} is the number of over voltage violations.
- 3) Loss (kWh) is the total loss realized in the network.
- 4) N_{LTC} is the number of LTC tap operations.
- 5) N_{VR} is the number of VR tap operations.
- 6) $N_{total} = N_{LTC} + N_{VR}$ is the total number of legacy device operation.
- 7) V_{max} is the maximum voltage recorded in the system.
- 8) V_{min} is the minimum voltage recorded in the system.

The simultaion results are summarized in table-II for the four different operating conditions as per fig. 5. The key insights are summarized below:

Under all operating conditions the proposed VVO scheme (case-3) eliminates over voltage and under voltage issues indicated by the N_{UV} and N_{OV} values. Case-1 performs poorly as it can neither address the under voltage issues during peak load condition nor the over voltage issues during peak PV condition which indicates that the legacy devices are incapable of addressing voltage issues in presence of PV. Even though case-2 with fixed VVar-C is capable of drastically reducing these violations, it still cannot completely eliminate the violations. But case-2 still performs really well in eliminating the over-voltage issues caused by PV as highlighted in the results of light load operating conditions.

Another major advantage of the proposed VVO scheme is the significant reduction in operation of legacy devices. In case-1 the overall operation of LTC and VR is significantly high since in the absence of smart inverter capability, all the intermittency in PV is handled by the legacy devices. The VR operations are higher than LTC due to the time delay between them. On the other hand, case-2 manages to reduce the overall tap operations from case-1 but still the N_{total} is significantly high due to lack of coordination between the inverter control and legacy device control. Moreover, even with such high tap operations both the cases perform poorly in eliminating the voltage issues. The proposed scheme manages to considerably reduce the overall number of tap operations while completely eliminating any voltage violations in the circuit. The reduction is extensively highlighted during cloudy PV days where proposed scheme reduces operation by about 90% compared to case-1 and 70% compared to case-2.

Since, in the proposed scheme we optimize the var injections for total power loss minimization, we can observe a considerable reduction in the total power loss realized during the 24 hour simulation. During high load condition we can

TABLE II
CASE STUDY COMPARISON UNDER DIFFERENT OPERATING CONDITIONS

Metrics	High Load						Light Load					
	Cloudy PV			Sunny PV			Cloudy PV			Sunny PV		
	Case-1	Case-2	Case-3	Case-1	Case-2	Case-3	Case-1	Case-2	Case-3	Case-1	Case-2	Case-3
N_{OV}	2	0	0	0	0	0	39	0	0	153	0	0
N_{UV}	228	74	0	219	75	0	0	0	0	0	0	0
Loss (kWh)	1373.02	1510.58	1189.07	1358.04	1542.39	1233.23	316.97	575.97	351.44	466.41	730.56	512.6
N_{LTC}	2	2	21	2	2	8	3	3	1	3	3	2
N_{VR}	629	284	106	253	68	47	372	106	12	56	27	21
N_{total}	631	286	127	255	70	55	375	109	13	59	30	23
V_{max}	1.056	1.025	1.05	1.05	1.025	1.05	1.062	1.03	1.043	1.058	1.027	1.048
V_{min}	0.909	0.9375	0.956	0.909	0.9375	0.951	0.952	0.963	0.964	0.954	0.963	0.956

see that the proposed scheme has the lowest loss compared to case-1 and case-2. Case-2 has particularly high loss because local control approach is known to increase the power loss due to lack of coordination in control between the inverters. This is also evident from case-1 loss which is lower than case-2 in the absence of inverter control. During light load condition the power loss of case-1 is lower than proposed scheme because the overall reactive load in the circuit is low and with inverter control in proposed scheme the loss is higher due to var injections from the smart inverters.

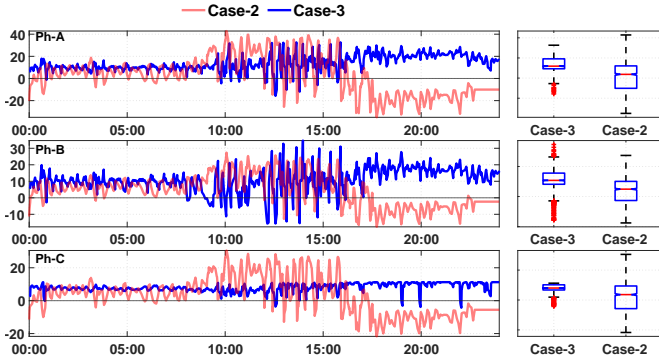


Fig. 7. Comparison of Reactive Power Injections from Inverter at node 840 for High Load Cloudy PV condition.

Figure 7 shows the reactive power injections from inverter at node 840 during high load cloudy PV condition between case-2 and case-3. In all three phases of the inverter case-3 manages to use very low var to regulate the voltage which leads to much less power loss as seen in table-II. This shows the advantage of shifting the curves compared to case-2.

Further investigation shows that by shifting the curves we are managing the reactive power requirements from the inverters strategically depending on size and location of the inverters on the circuit. As highlighted in fig. 8 the reactive power from the inverter at node 890 which has a large PV system in the middle of the circuit is utilized as conventional VVar-C device injecting reactive power at high load condition while inverters towards the end at node 836, 840, and 848 with comparatively lower size are operated as reactive power absorbing devices. While in case-2 the reactive power requirements are equally distributed among the inverters which all act as reactive power injecting devices during high load condition.

The voltage drop issue associated with absorbing reactive power during high load condition is mitigated by keeping the

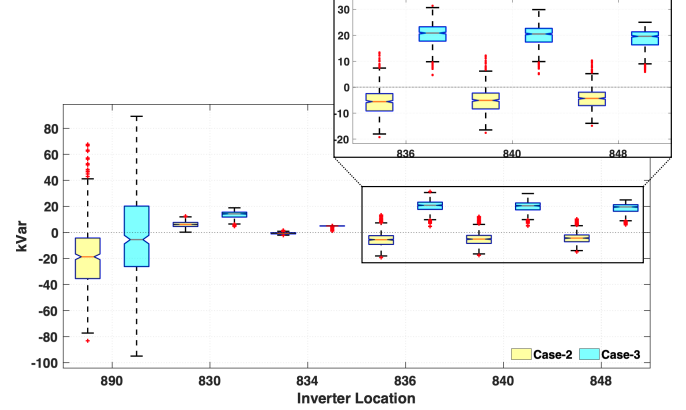


Fig. 8. Distribution of Reactive Power Injections from 16:00-24:00 for High Load Cloudy PV Condition.

LTC taps at maximum position as shown in fig. 9 compared to case-2 and case-1. This also highlights the advantage of coordinated control between the devices.

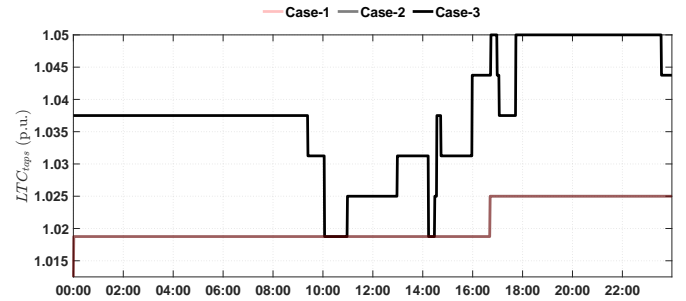


Fig. 9. LTC tap change for High Load Cloudy PV condition

Apart from the reduction in the reactive power usage, the main advantage of shifting the VVar-C is the smoothing of system voltage profile. Figure 10 shows the distribution of voltage at end node 840, which shows that proposed case has a much tighter voltage profile compared to case-2. This is beneficial to utilities while applying conservation voltage reduction (CVR).

To validate the claim that by shifting the curve the equilibrium point of new curve is in fact the optimal solution from central VVO problem we show the error between the optimal var command against the var injection from new curve for same operating points at 5-min intervals in fig. 11. We can

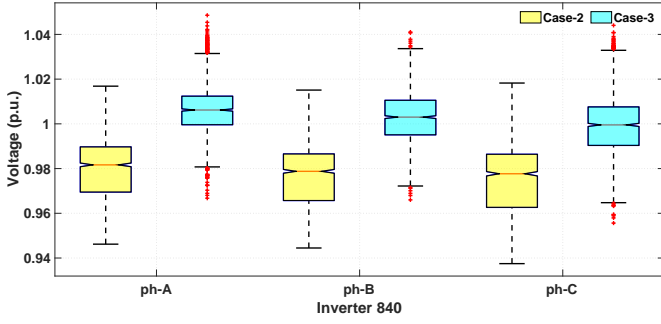


Fig. 10. Comparison of 24h Voltage Profile at End Node 840 for High Load Cloudy PV condition

see that the error is very low about 7% average which is predominantly from the accumulation of inherent steady state error of Volt/VAR curves from all inverters in the system which leads to a maximum voltage error of only 0.4%.

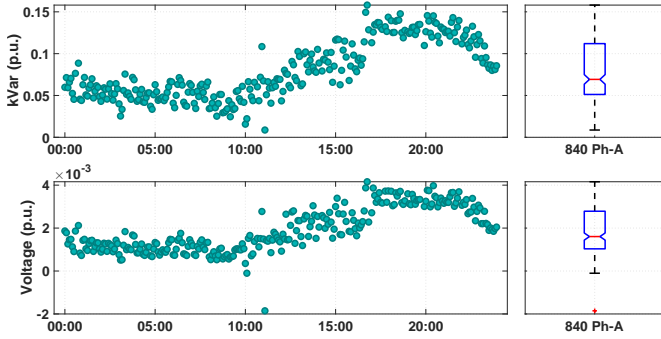


Fig. 11. Error in reactive power injections (*top*) and measured voltage (*bottom*) vs optimal command at inverter 840 on phase-A at 5-min control intervals.

Time taken for optimization problem to converge at every 5-minute interval is shown in fig. 12. Under all operating conditions the maximum time taken to converge is only 1 sec which indicates that the proposed algorithm can easily be applied to larger systems with multiple voltage regulators and smart inverters while still dispatching with 5-min control interval.

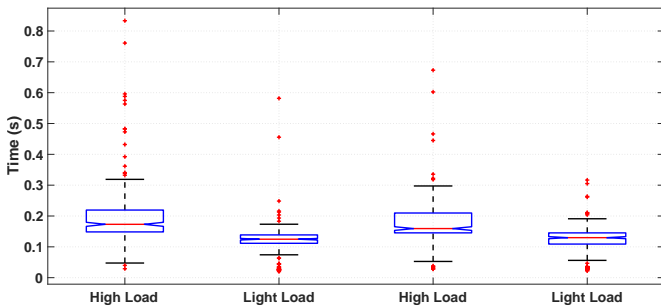


Fig. 12. Time taken for Two-Stage Optimization Problem to Converge

IV. CONCLUSION

This paper proposes a new Volt/VAR optimization (VVO) scheme that coordinates the control of legacy devices like

voltage regulators and load tap-changers with smart inverters for real-time implementation. A new dispatching scheme for smart inverters is proposed that utilizes the optimal var injections obtained from the coordinated VVO to shift the existing volt/var curves in the inverters laterally thereby minimizing the communication requirement as well as reduce the dependency on centralized VVO for voltage regulation. Simulation results on a test feeder shows that the new VVO is superior to conventional volt/var control schemes based on local measurements in eliminating the voltage violations, provide better voltage regulation, significant reduction in tap operation which will reduce the wear and tear of the mechanical devices, and overall reduction in power loss in the circuit.

REFERENCES

- [1] ANSI C84.1-2020 - Electric Power Systems and Equipment - Voltage Ratings (60 Hz). [Online]. Available: <https://webstore.ansi.org/Standards/NEMA/ANSIC842020>
- [2] V. Sharma, S. M. Aziz, M. H. Haque, and T. Kauschke, "Effects of high solar photovoltaic penetration on distribution feeders and the economic impact," vol. 131, p. 110021. [Online]. Available: <https://www.sciencedirect.com/science/article/pii/S1364032120303129>
- [3] "IEEE Standard for Interconnection and Interoperability of Distributed Energy Resources with Associated Electric Power Systems Interfaces," pp. 1–138.
- [4] A. Singhal, V. Ajjarapu, J. Fuller, and J. Hansen, "Real-Time Local Volt/Var Control Under External Disturbances With High PV Penetration," vol. 10, no. 4, pp. 3849–3859. [Online]. Available: [10/gjnrs3](https://doi.org/10/gjnrs3)
- [5] Rule 21 Interconnection Standard, CA. [Online]. Available: <https://www.cpuc.ca.gov/rule21/>
- [6] P. Jahangiri and D. C. Aliprantis, "Distributed Volt/VAR Control by PV Inverters," vol. 28, no. 3, pp. 3429–3439.
- [7] T. Ding, K. Sun, C. Huang, Z. Bie, and F. Li, "Mixed-Integer Linear Programming-Based Splitting Strategies for Power System Islanding Operation Considering Network Connectivity," vol. 12, no. 1, pp. 350–359. [Online]. Available: [10/gfmffq](https://doi.org/10/gfmffq)
- [8] E. Dall'Anese, S. V. Dhople, and G. B. Giannakis, "Optimal Dispatch of Photovoltaic Inverters in Residential Distribution Systems," vol. 5, no. 2, pp. 487–497.
- [9] M. Farivar, Lijun Chen, and S. Low, "Equilibrium and dynamics of local voltage control in distribution systems," in *52nd IEEE Conference on Decision and Control*. IEEE, pp. 4329–4334. [Online]. Available: <http://ieeexplore.ieee.org/document/6760555/>
- [10] B. A. Robbins and A. D. Domínguez-García, "Optimal Reactive Power Dispatch for Voltage Regulation in Unbalanced Distribution Systems," vol. 31, no. 4, pp. 2903–2913.
- [11] W. Xu, Q. Tang, T. Li, Y. Lei, F. Liu, Z. Jia, Y. Xiang, J. Liu, and S. Jawad, "Optimal Investment of Mobile Energy Storage Based on Life Cycle Cost-benefit Analysis," in *2019 IEEE 3rd Conference on Energy Internet and Energy System Integration (EI2)*, pp. 508–513. [Online]. Available: [10/gjg9kz](https://doi.org/10/gjg9kz)
- [12] R. R. Jha, A. Dubey, C.-C. Liu, and K. P. Schneider, "Bi-Level Volt-VAR Optimization to Coordinate Smart Inverters With Voltage Control Devices," vol. 34, no. 3, pp. 1801–1813. [Online]. Available: <https://ieeexplore.ieee.org/document/8598813/>
- [13] M. Manbachi, A. Sadu, H. Farhangi, A. Monti, A. Palizban, F. Ponci, and S. Arzanpour, "Real-time communication platform for Smart Grid adaptive Volt-VAR Optimization of distribution networks," in *2015 IEEE International Conference on Smart Energy Grid Engineering (SEGE)*, pp. 1–7.
- [14] R. Neal and R. Bravo, "Advanced Volt/VAR control element of Southern California Edison's Irvine smart grid demonstration," in *2011 IEEE/PES Power Systems Conference and Exposition*, pp. 1–3.
- [15] V. Muthukaruppan and M. E. Baran, "AMI Based Communication Scheme for Decentralized Volt/VAR Control," in *2020 IEEE Power & Energy Society General Meeting (PESGM)*, pp. 1–5.
- [16] B. Zhang, A. Y. Lam, A. D. Domínguez-García, and D. Tse, "An Optimal and Distributed Method for Voltage Regulation in Power Distribution Systems," vol. 30, no. 4, pp. 1714–1726.

- [17] W. Zheng, W. Wu, B. Zhang, H. Sun, and Y. Liu, "A Fully Distributed Reactive Power Optimization and Control Method for Active Distribution Networks," vol. 7, no. 2, pp. 1021–1033.
- [18] M. Bazrafshan, N. Gatsis, and H. Zhu, "Optimal Power Flow With Step-Voltage Regulators in Multi-Phase Distribution Networks," vol. 34, no. 6, pp. 4228–4239.
- [19] G. Ozdemir, S. Emiroglu, and M. Baran, "Supervisory control for coordinating Volt/Var control devices on a distribution system," in *2016 IEEE Power & Energy Society Innovative Smart Grid Technologies Conference (ISGT)*, pp. 1–5.
- [20] X. Zhou, M. Farivar, Z. Liu, L. Chen, and S. H. Low, "Reverse and Forward Engineering of Local Voltage Control in Distribution Networks," vol. 66, no. 3, pp. 1116–1128.
- [21] T. A. Short, *Electric Power Distribution Handbook*, ser. Electric Power Engineering Series. Boca Raton, FL : CRC Press, [2004]. [Online]. Available: <https://catalog.lib.ncsu.edu/catalog/NCSU1661527>

APPENDIX

A. Proof of Theorem-II.1

Proof. Let $g(v, q) = 0$ denote the 3-phase power flow solution of an unbalanced distribution system.

Let $q = f(v - v_{ref})$ denote the volt/var control function where $f: \mathbf{R}^n \rightarrow \Omega$ denote the set of individual inverter volt/var functions $f_i: \mathbf{R} \rightarrow \Omega_i$. Note that $q \in \Omega = \prod_{i=1}^n \Omega_i$ where, $\Omega_i = \{q_i \mid \underline{q}_i \leq q_i \leq \bar{q}_i\}$ is determined by the inverter limits. Generally, \underline{q}_i is 0 and \bar{q}_i is the available reactive power determined by the current real power output and inverter size.

A point (v^*, q^*) is an equilibrium point of control function f if it satisfies the following equations [20]:

$$\begin{aligned} g(v^*, q^*) &= 0 \\ q^* &= f(v^* - v_{ref}) \end{aligned} \quad (7)$$

Given an optimal power flow solution (v_g, q_g) which implies $g(v_g, q_g) = 0$. This point will not be an equilibrium point of f but we can still find a voltage v_l corresponding to q_g since $q_g \in \Omega$ as the inverter limits are included as a constraint in optimal power flow problems. This implies $v_l = f^{-1}(q_g)$ or $q_g = f(v_l - v_{ref})$, note that f^{-1} exist since f is non-increasing. (v_l, q_g) will not be an equilibrium point since it does not solve the power flow equations, $g(v_l, q_g) \neq 0$.

By shifting the function f along the voltage axis by $v_g - v_l$ we have,

$$\begin{aligned} q_g &= f(v_l - v_{ref} + v_g - v_l) \\ q_g &= f(v_g - v_{ref}) \end{aligned} \quad (8)$$

which shows that (v_g, q_g) is a solution of the shifted function $f(v - v_{ref} + v_g - v_l)$ and it is also the equilibrium point of the system since it satisfies the power flow equations $g(v_g, q_g) = 0$. The direction of shift will be implicitly taken care by the sign of $v_g - v_l$.

This shows that the an optimal inverter set point can be dispatched to inverters without modeling the volt/var curves in the optimal power flow problem which can become computationally intensive. There are no restrictions on the volt/var curve f and the optimal power flow problem, so any objective can be utilized and the volt/var function f can be continuously shifted by using the previous curve information. \square



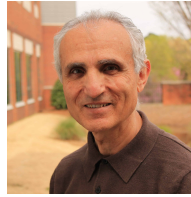
Valliappan Muthukaruppan (S'17) received the B.Tech degree in electrical engineering from National Institute of Technology, Trichy, India in 2014, and the M.S. degree in electrical engineering from North Carolina State University, Raleigh, NC, USA in 2018. He is currently working towards the Ph.D. degree in electrical engineering at North Carolina State University.

His research interests include application of optimization, data science, and machine learning techniques to control and operate smart distribution networks with high renewable penetration.



Yue Shi (S'12-M'18-SM'19) received the B.E. degree in electrical engineering from Tianjin University, Tianjin, China, in 2012, the M.S. and Ph.D. degree in electrical engineering from North Carolina State University, Raleigh, NC, USA in 2014 and 2018.

Her research interests include Volt/Var optimization, electric utility asset investment optimization, and impacts of renewable energy and electric vehicles on power distribution systems.



Mesut E. Baran (S'87-M'88-SM'05-F'11) received the B.S. and M.S. degree from Middle East Technical University, Ankara, Turkey, and the Ph.D. degree from the University of California, Berkeley, CA, USA, all in electrical engineering. He is currently a Professor with North Carolina State University, Raleigh, NC.

His research interests include distribution and transmission system analysis and control, integration of renewable energy resources, and utility applications of power electronics based devices. He is currently a member of the FREEDM Systems Center with North Carolina State University focusing on both research and education aspects of renewable electric energy systems and their integration in to the electric power distribution system.